

Synthesis and Anticancer Activity of Polymer Nanocomposites with Moringa- Extracted CuO and Ag₂O Nanoparticles

Sarah Saadi Ahmed*¹, Nada Abbass²

Abstract

Background: This study aimed to synthesize copper oxide (CuO) and silver oxide (Ag₂O) nanoparticles using a green synthesis method involving moringa extract and incorporate them into polymer nanocomposites with polyacrolein. The objective was to evaluate their cytotoxicity against fibroblasts and glioblastoma cell lines.

Methods: The CuO and Ag₂O nanoparticles were synthesized using moringa extract as a reducing agent. Nanocomposites were formed through a condensation reaction with polyacrolein. Characterization techniques included Atomic Force Microscopy (AFM), Fourier Transform Infrared Spectroscopy (FT-IR), Transmission Electron Microscopy (TEM), X-Ray Diffraction (XRD), Thermogravimetric Analysis (TGA), and Differential Scanning Calorimetry (DSC). Cytotoxicity was evaluated through in vitro assays using human dermal fibroblasts (HdFn) and A172 glioblastoma cells.

Results: AFM analysis showed nanoparticle sizes of 19.36 nm for Ag₂O and 66.89 nm for CuO, while TEM images revealed nonhomogeneous spherical nanocomposites. FT-IR and XRD confirmed the successful incorporation of nanoparticles into the polymer matrix. TGA and DSC results demonstrated thermal stability and transitions of the nanocomposites. Cytotoxicity assays indicated significant inhibition of A172 glioblastoma cell proliferation with minimal impact on normal fibroblast cells, suggesting selective cytotoxicity.

Conclusion: The polymer nanocomposites incorporating moringa-extracted CuO and Ag₂O nanoparticles exhibited promising selective cytotoxicity against glioblastoma cells, indicating their potential use as anticancer agents. Further studies on in vivo applications and long-term stability are warranted to advance their biomedical use.

Keywords: Antineoplastic Agents, Copper Oxide, Cytotoxicity, Green Chemistry Technology, Moringa oleifera, Polyacrolein, Polymer Nanocomposites, Silver Oxide.

Introduction

Nanotechnology has revolutionized the development of materials with extraordinary properties and functionalities in the field of material science. Among those, metal oxide nanoparticles have received enormous attention because of their unique optical, electrical, and catalytic properties. These have developed lately for application in biomedical, environmental, and industrial fields, among

others. Basically, the potential of metal oxide nanoparticles in the treatment of cancer has been the subject of reasonable interest because such particles can interact with the biological system at a molecular level, thereby opening new avenues for targeted and effective treatments (1, 2).

Another critical area of research in nanotechnology is the synthesis of

1: Department of Chemistry, College of Science, University of Baghdad, Baghdad, Iraq.

2: Clinical Research Unit, University of Medical Sciences, Baghdad, Iraq.

*Corresponding author: Sarah Saadi Ahmed; Tel: +96 47716614067; E-mail: sara94sadi@gmail.com.

Received: 9 Aug, 2024; Accepted: 21 Dec, 2024

nanoparticles through environmentally friendly routes, popularly known as green syntheses. Green synthesis uses biological systems and plant-based materials to synthesize nanoparticles that are safe, cost-effective, and non-toxic to the environment. This sharply contrasts with the conventional chemical route, which involves hazardous chemicals and often yields toxic byproducts (3, 4). The impact on both the environment and human health from traditional methods of synthesis is the reason for finding alternative techniques that work in accordance with sustainability.

Recent literature has exposed the potentials of plant extracts toward metal oxide nanoparticle biosynthesis. For instance, *Glycyrrhiza glabra* was utilized in the synthesis of Cr_2O_3 nanoparticles because of its medicinal properties. In the same manner, *Moringa oleifera*, recognized by several health benefits, has been used in this study to synthesize CuO and Ag_2O nanoparticles (5). The nanoparticles alone, in association with other polymers, frequently form improved nanocomposites with a variety of applications in the field of anticancer therapies. Among the various polymeric materials that can be used to create nanocomposites with metal oxide nanoparticles, the unique properties of polyacrolein mechanical strength, thermal stability, and chemical resistance—make it an excellent candidate.

Thus, the prime objectives of the present study are the synthesis of CuO and Ag_2O nanoparticles using *Moringa* extract and the preparation of nanocomposites of these nanoparticles into polyacrolein, followed by detailed studies of their structural, thermal, and biological properties. This will describe modern synthesis combined with advanced nanocomposite formation to develop potential anticancer materials. This work shall present a comprehensive cross-sectional overview regarding synthesis, characterization, and possible biomedical applications of such newly developed nanocomposites.

Materials and Methods

Polyacrylonitrile was procured from SABIC Company. Cupric (II) Chloride nonahydrate ($\text{CuCl}_2 \cdot 9\text{H}_2\text{O}$), silver nitrate (AgNO_3), and moringa leaves were sourced from local markets in Baghdad, Iraq.

Extraction of Moringa Leaf

The dried roots of moringa were ground, and 2 grams of the powder was added to 50 mL of distilled water. The mixture was heated to the boiling point and then cooled to room temperature. The resulting solution was filtered multiple times using gauze to obtain the aqueous extract.

Biosynthesis of Metal Oxide Nanoparticles

Cupric (II) Chloride nonahydrate (0.7 mg) and silver nitrate (0.7 mg) were each dissolved in a small amount of distilled water. The moringa extract was gradually added to each solution under gentle heating and stirring. A change in the color of the solutions indicated the formation of nanoparticles, which were then dried in an oven at 80°C (6).

Preparation of Nanocomposite

In a round-bottomed flask, 5 grams of isotactic polypropylene was dissolved in 20 mL of Dimethyl Sulfide by heating at 90°C . Metal oxide nanoparticles were added to the solution in a 1:5 ratio of nanoparticles to polyacrolein. The mixture was stirred for an hour to ensure homogeneity. The reaction mixture was then transferred to a petri dish and dried in an oven at 80°C to remove residual solvent, resulting in the formation of the nanocomposite.

Results

AFM Analysis of Metal Oxide Nanoparticles

Atomic Force Microscopy (AFM) was used to determine the topography and surface morphology of the synthesized Ag_2O and CuO nanoparticles. The AFM images revealed heterogeneous grooves due to nanoparticle agglomeration see (Figs. 1 & 2). The particle diameters were found to be 19.36 nm for Ag_2O and 66.89 nm for CuO ,

indicating successful synthesis with desirable nanoscale dimensions (Tables 1 & 2).

Table 1. Dimensions of Ag₂O nanoparticles synthesis was measured using surface morphology.

Statistic	Particle Area (nm ²)	Particle Diameter (nm)	Particle Height (nm)
Mean	10,151	66.89	82.20
Min	4,357	4.612	75.82
Max	224,045	506.3	134.0

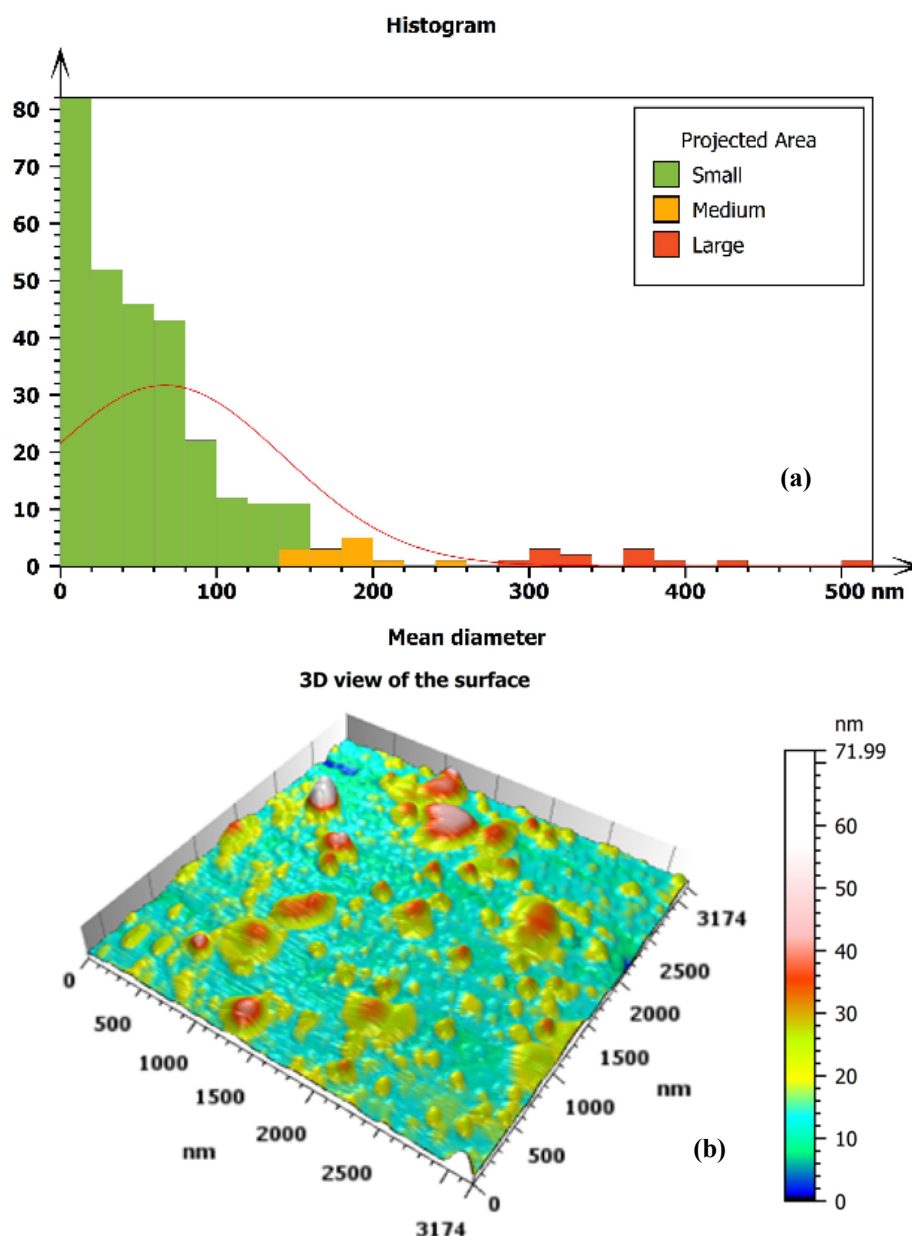


Fig. 1. (a) 3D Atomic Force Microscopy (AFM) image of Ag₂O nanoparticles showing surface topography and morphology, indicating heterogeneous grooves due to nanoparticle agglomeration. (b) Granularity cumulation distribution chart for Ag₂O nanoparticles, displaying particle size distribution and frequency.

Table 2. Dimensions of Ag₂O nanoparticles synthesis were measured using surface morphology.

Statistic	Particle Area (nm ²)	Particle Diameter (nm)	Particle Height (nm)
Mean	1,230	19.36	42.72
Min	5.096	1.577	32.42
Max	62,437	333.2	89.49

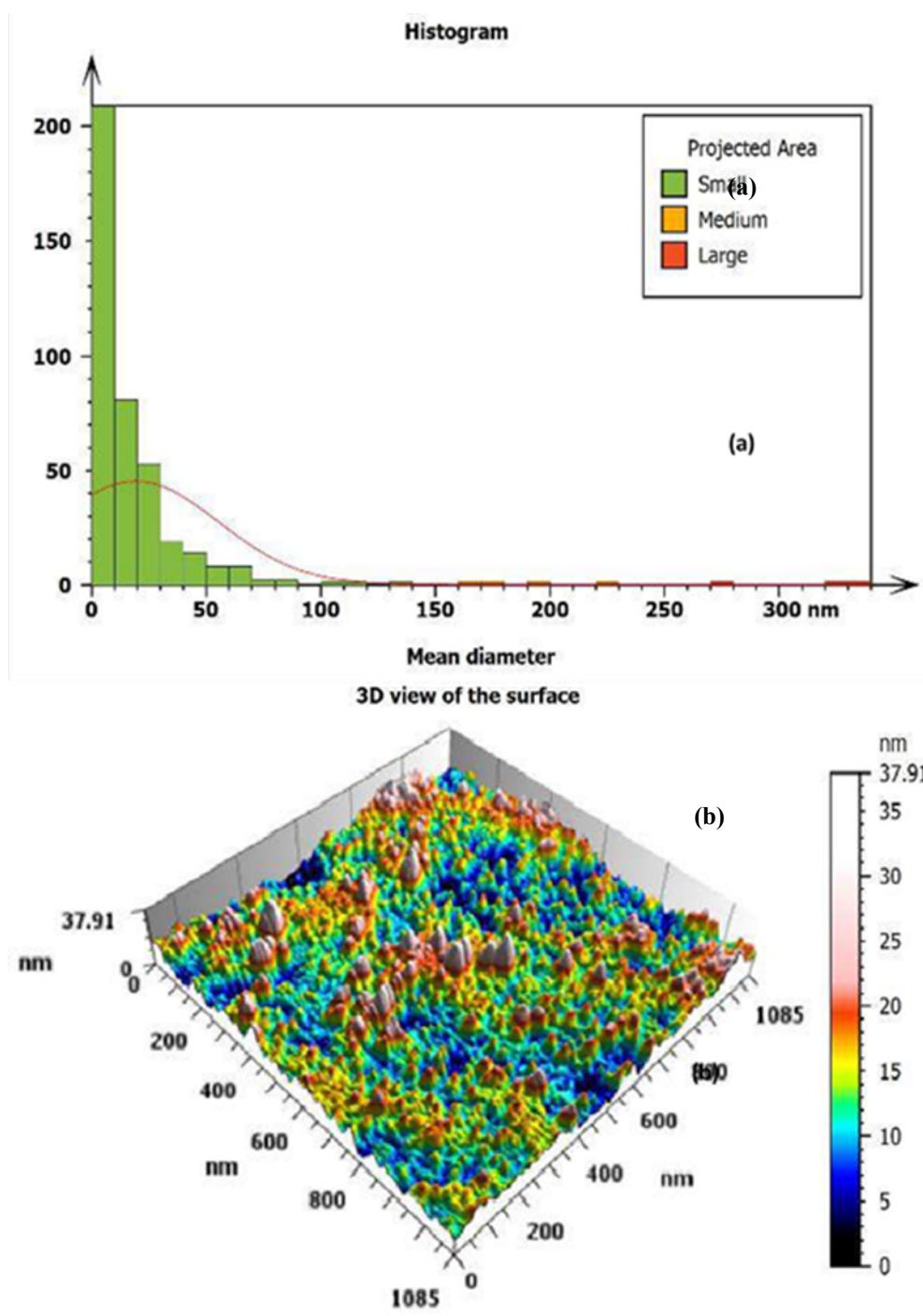


Fig. 2. (a) Granularity cumulation distribution chart for CuO nanoparticles, illustrating the distribution of particle sizes and their relative frequency. (b) 3D Atomic Force Microscopy (AFM) image of CuO nanoparticles, revealing surface topography with characteristic grooves due to agglomeration.

The particle sizes obtained in this study are comparable to those reported in the literature. For example, Al-Shaheen et al. (4) reported the synthesis of ZnO nanoparticles with diameters ranging from 20 to 70 nm using similar green synthesis techniques. The consistency in particle size is crucial as it impacts the surface area and reactivity of the nanoparticles, which are important factors for their biological applications.

TEM Analysis of Nanocomposites

Transmission electron microscopy was used for the morphological studies of nanocomposites. CuO, as well as Ag₂O nanocomposites were in polyacrylonitrile matrices, and the morphologies were not so homogeneous spherical in general terms. Apparently, it also showed nanoparticles over the polymer matrix and therefore not incredibly homogenous. Previously, these phenomena had been verified by similar studies, for example, Ramazanov and Hajiyeva (11). The morphology of the nanoparticles and their dispersion in the polymer matrix becomes important factors strongly influencing the mechanical, thermal, and biological performance of the nanocomposites.

The non-homogeneous spherical morphology of both types of nanocomposites described herein is most probably the result of different degrees of interaction with the used polymer (Fig. 3). This, in turn, supports the findings that the most cardinal attributes that govern the properties of the composite are the dispersion and interaction of the nanoparticles within the matrix.

Such results are consistent with those reported by Ramazanov and Hajiyeva (11): they also wrote about the importance of the nanoparticle morphology and dispersion in the creation of the properties of nanocomposites. Therefore, it is noted that

these differences in the properties of the interaction of nanoparticles with polymers generally lead to morphological differences and total performance differences after the preparation of nanocomposites.

This contrasts with the research using TEM images by Almarbd and Abbass, where it was vivid that the (PS/GO/Ag₂O) and (PS/TiO₂/Ag₂O) nanocomposites were well dispersed in the polystyrene matrix. This favoured even spreading of the nanoparticles and resulted in the improved mechanical and biological properties of the nanocomposites (12).

In contrast to the above, the TEM images of this study exhibit a spherical, non-homogeneous morphology, very likely representing a lower degree of uniformity on the distribution of the nanoparticles into the polyacrylonitrile matrix compared to prior works. The differences in their morphologies and dispersions may reflect the differences in synthesis methods and the types of polymeric matrices themselves. While Almarbd and Abbass synthesized nanoparticles by a method of green synthesis and used a simple mixing process for nanoparticles incorporation, this study adopted a different methodology approach that made the differences in nanoparticle dispersion and interaction. The findings of Almarbd and Abbass's research also matched the current results as the relative improvement in the nanocomposites can only be achieved with an even dispersion of nanoparticles in the matrices for their improved mechanical and biological performance. These relative insights underline the importance of optimal synthesis practices in obtaining required nanoparticle dispersion and interaction within polymer matrices, hence improving the performance of the nanocomposite materials (Fig. 3).

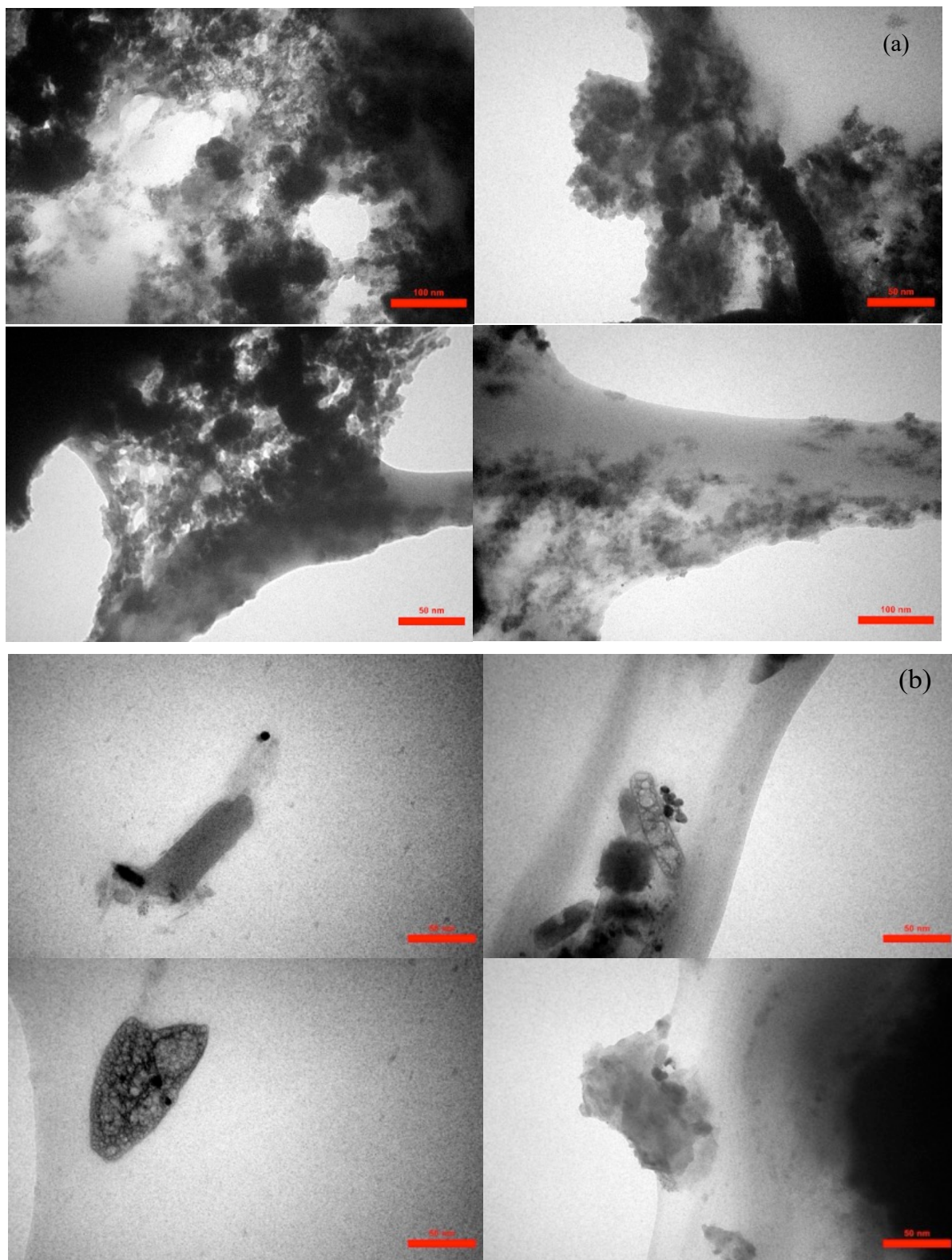


Fig. 3. Transmission Electron Microscopy (TEM) images of nanocomposites: (a) TEM image of the CuO nanocomposite, illustrating the dispersion and interaction of CuO nanoparticles within the polyacrylonitrile matrix. The non-homogeneous spherical morphology suggests varying degrees of interaction with the polymer, impacting the overall properties of the composite material. (b) TEM image of the Ag₂O nanocomposite, showing the dispersion of Ag₂O nanoparticles within the polyacrylonitrile matrix. The observed morphology reflects differences in nanoparticle dispersion and interaction, influenced by the synthesis method and polymer compatibility (the size of Red bar is 50 nm).

FT-IR Spectroscopy of PA Composites

Fourier Transform Infrared Spectroscopy (FT-IR) analysis showed characteristic absorption bands for polypropylene and nanoparticle composites, which confirmed the successful synthesis of nanocomposites. The existence of different absorption bands at 3441 and 3385 cm^{-1} corresponds to the OH group stretching; 2961, 2924, and 2841 cm^{-1}

correspond to aliphatic C-H stretching; and 1460 cm^{-1} corresponds to CH₂ deformation, NO - M, Cu - O showing a strong polymer-nanoparticle matrix formulation. These bands confirm the chemical interactions between the polymer matrix and the nanoparticles, thus explaining the stability and functionality of the nanocomposites (Fig. 4).

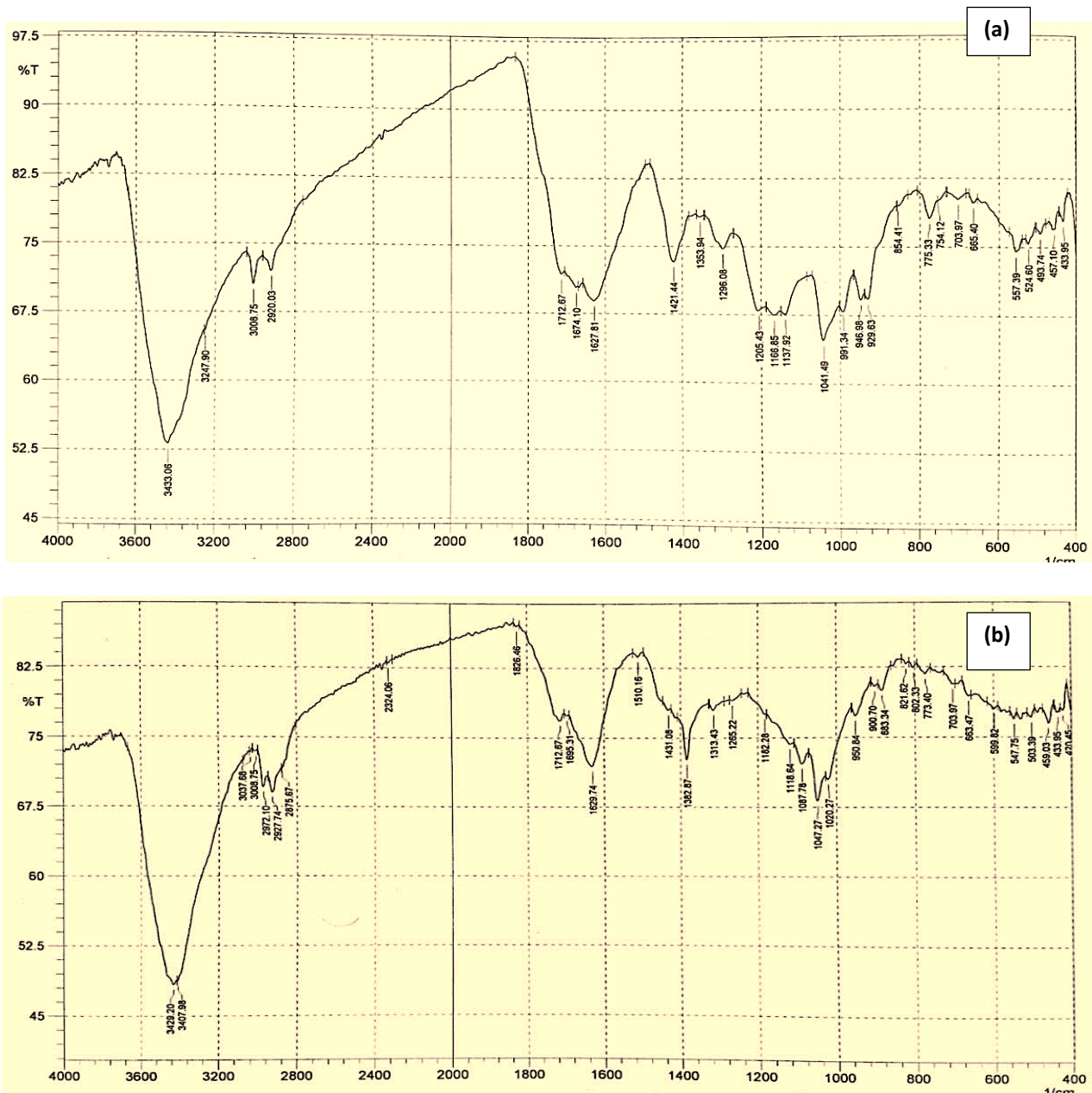


Fig. 4. (a) FT-IR Spectrum of the PA/CuO nanoparticle composite, showing characteristic absorption bands for OH stretching (3441 and 3385 cm^{-1}), aliphatic C-H stretching (2961, 2924, and 2841 cm^{-1}), and CH₂ deformation (1460 cm^{-1}), indicating successful incorporation of CuO nanoparticles into the polymer matrix. (b) FT-IR Spectrum of the PA/Ag₂O nanoparticle composite, highlighting similar absorption bands along with additional peaks corresponding to NO-M and Cu-O interactions, confirming strong chemical bonding and interaction between Ag₂O nanoparticles and the polymer matrix.

These results are in good agreement with those from Jung et al. (17), who also witnessed these features of the FT-IR spectra in their studies on polymer-based nanocomposites. FT-IR analysis is critical for spelling out the functional groups involved in the synthesis process and confirms the successful inclusion of nanoparticles into the polymer matrix.

X-Ray Diffraction (XRD) of PP Composites

The XRD pattern consisted of peaks related to pure polypropylene and the phases of metal oxide, which proved that CuO and Ag₂O nanoparticles were successfully integrated into the matrix of polypropylene. Data obtained give some idea about the structural integrity and phase composition of these nanocomposites, which are very important in their application (Table 4 & Fig. 5).

Table 4. XRD Analysis of PP Nanocomposites.

2 θ (Degree)	FWHM (Degree)	dhkl (Å)	G.S (nm)	Phase	hkl
13.8675	0.7417	6.1845	11.5	PP	110
16.8344	0.6887	5.1563	13.5	PP	040
18.3709	0.6887	4.7242	12.5	PP	130
21.8675	1.3245	4.0301	10.2	PP	111
25.2053	0.6887	3.4696	13.7	PP	060
28.543	1.3245	3.1000	9.2	PP	220
32.7362	1.2004	2.7350	14.8	CuO	111
38.7263	1.3002	2.3225	13.2	Ag ₂ O	200

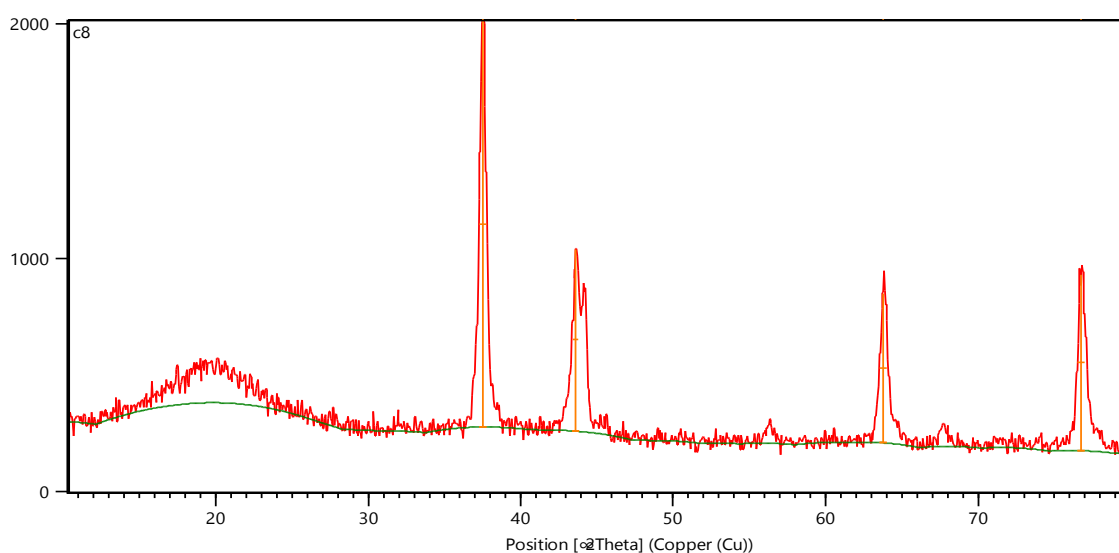


Fig. 5. X-Ray Diffraction (XRD) pattern of the PP/Ag₂O nanoparticle composite, displaying diffraction peaks corresponding to polypropylene (PP) phases and the integrated metal oxides (CuO and Ag₂O). The peaks at 2 θ values of 32.736° and 38.726° confirm the presence of CuO (111) and Ag₂O (200) phases, respectively, while other peaks correspond to the crystalline phases of polypropylene.

The crystallographic data are in good agreement with those reported by Zoromba et al. (20), who studied almost the same nanocomposites and noticed very similar

patterns of diffraction. Hence, XRD analysis plays a vital role in the formation of these nanocomposites and explains their structural properties.

Thermogravimetric Analysis (TGA) and Differential Scanning Calorimetry (DSC)

TGA gave the different thermal degradation stages of the nanocomposites, whereas DSC gave information about the glass transition and melting points of the polypropylene nanocomposites. The obtained TGA curve

shows that there are obviously three different stages of weight loss corresponding to adsorbed water loss, organic matter decomposition, and polymer matrix decomposition in both CuO and Ag₂O nanocomposites (Fig. 6a).

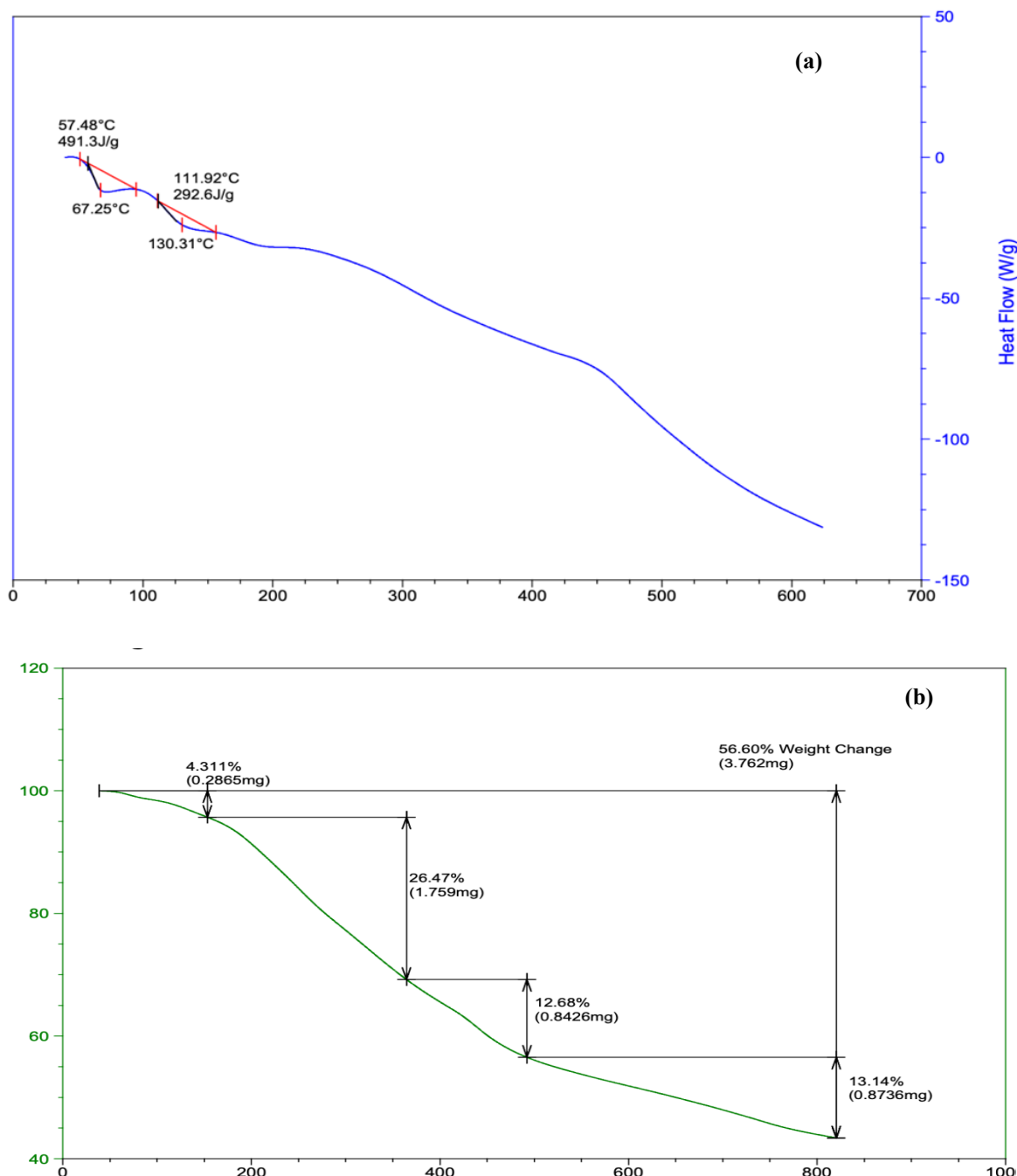


Fig. 6. (a) Differential Scanning Calorimetry (DSC) curve of PP/CuO and PP/Ag₂O nanocomposites, illustrating the glass transition temperature (T_g) and melting point (T_m). The glass transition temperature for PP/CuO is approximately 243.95 °C, with a melting point of 415.41 °C, indicating the successful thermal integration of CuO nanoparticles into the polymer matrix. (b) Thermogravimetric Analysis (TGA) curve of PP/CuO and PP/Ag₂O nanocomposites, showing three distinct stages of weight loss: water desorption, organic matter decomposition, and polymer matrix degradation. These stages confirm the thermal stability and decomposition characteristics of the nanocomposites.

The DSC analysis indicates that for CuO nanocomposites, the glass transition temperature is about 243.95 °C and a melting point of 415.41 °C. The Ag₂O nanocomposites show similar thermal transitions; this, therefore, proves the successful incorporation of these nanoparticles within the polymer matrix (Fig. 6b).

These thermal analysis results are in good accordance with those reported by Al-Husseini et al. (16) for nanocomposite materials that show such kinds of thermal behaviors. The addition of nanoparticles did not contribute to the thermal properties of the polymer matrix;

on the contrary, it proved the stability and solidity of synthesized nanocomposites. The TGA and DSC analyses give crucial information about the thermal stability and phase transitions of the nanocomposites relevant for practical applications.

Analysis of Concentrations on HdFn and A172 Cell Lines

The anticancer activity of the synthesized nanocomposites is evaluated by considering their effects on human dermal fibroblasts and glioblastoma cell lines at different concentrations.

Table 5. Effects of CuO and Ag₂O Nanoparticles on HdFn and A172 Cell Lines.

Concentration (µg/mL)	Cell Line	Mean (CuO)	SD (CuO)	Mean (Ag ₂ O)	SD (Ag ₂ O)
400	HdFn	74.653	2.577875	79.28233	1.1575
	A172	37.809	1.881804	42.978	4.462131
200	HdFn	86.34267	1.531323	86.45833	1.64081
	A172	43.17133	1.13998	51.659	2.98794
100	HdFn	93.59567	2.100082	90.62533	0.834408
	A172	54.89967	1.093744	59.68367	1.540952
50	HdFn	94.174	1.571414	94.02	0.770839
	A172	64.04333	2.150515	73.95833	1.728466
25	HdFn	95.216	0.820906	95.79467	0.267313
	A172	77.08333	2.23531	86.72833	1.300763

The data show that the synthesized nanocomposites insignificantly inhibited the proliferation of A172 cancer cells and had a minimal effect on HdFn normal cells (Table 5 & Fig. 7). These nanocomposites would, therefore, be selectively cytotoxic to

the cancer cells, making them a potential candidate for anti-cancer therapy. The selective cytotoxicity has been one of the prime factors in developing effective therapy with minimum damage to healthy cells.

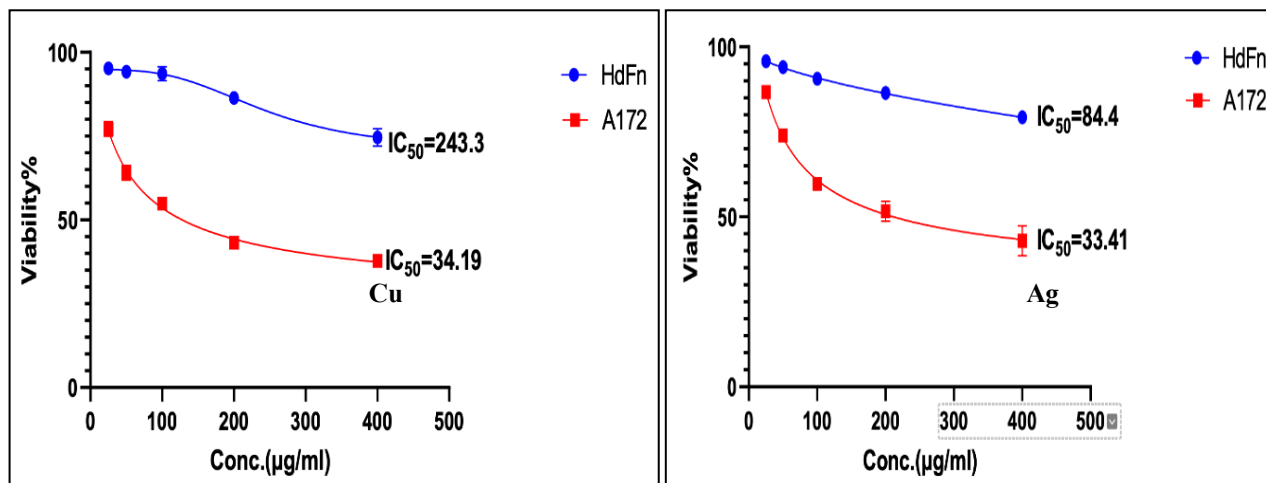


Fig. 7. Concentration effects of PP/CuO and PP/Ag₂O nanocomposites on HdFn (normal human dermal fibroblasts) and A172 (glioblastoma cancer cells) cell lines. The data demonstrate minimal proliferation inhibition in HdFn cells and selective cytotoxicity against A172 cells, highlighting the potential of these nanocomposites as candidates for targeted anti-cancer therapy.

The observed effects of nanocomposites on cell lines further interpreted in relation to their potential anticancer properties. The results suggest that the synthesized nanocomposites could be effective in cancer therapy due to their significant inhibition of cancer cell proliferation at different concentrations. The level of inhibition of the synthesized nanocomposites points to a broad spectrum of biological activity for metal oxide nanoparticles in the antifungal effect of silver nanoparticles reported against various pathogenic fungi by Kim et al. (21).

The nanocomposites synthesized for this study exhibit rather selective cytotoxicity against the A172 glioblastoma cell line, with minimal effects against the HdFn human dermal fibroblast cell line. This could be attributed to the fact that normal and malignant cells exhibit differences in metabolic activity or membrane properties. Normally, cellular metabolism is altered in cancerous cells due to a higher proliferation rate compared with normal cells, which renders the former more vulnerable to the oxidative stress caused by the synthesized nanocomposites.

These nanocomposites exert their biological effects through multiple mechanisms, one of which is the generation of ROS, resulting in an overall situation of oxidative stress. This results in more harm to

cancer cells since they are in a stage of accelerated metabolic activity and might induce programmed cell death or apoptosis. The induction of apoptosis is a hallmark of anticancer activity that selectively kills cancer cells and spares normal ones. It can also result in interactions of nanoparticles with the cell membrane, leading to structural damage, changed permeability, and perturbation of key cellular functions, that might turn out to be more deleterious in cancer cells due to the differences in their composition.

Another possible reason could be the difference in uptake and accumulation of nanoparticles in the two used cell lines, HdFn and A172. In cancer cells, such as in the A172 cell line, endocytosis is increased, allowing for an increase in cellular uptake of nanoparticles and intracellular concentrations, thereby increasing the cytotoxicity. This metal ion release, particularly Ag⁺ ions from Ag₂O, is believed to be a driving force behind the observed cytotoxic effects. These ions are known to exert antimicrobial properties and have been reported to interfere with cellular functions, including the activity of enzymes and the integrity of membranes. This is a differential sensitivity of normal and cancer cells toward such ions, which underlines the selective cytotoxicity observed.

It may further influence specific cellular pathways in normal and cancerous cells. For example, it may inhibit several pathways to survival and proliferation of cancer cells, mediated by growth factors or angiogenesis, while possibly supporting normal cellular functions. The multifaceted mechanism of action thus labels the nanocomposites as potential candidates for further research in the realms of cancer therapy. These results are, therefore, indicative of a wide spectrum of biological activity. Observations corresponding to the already known antimicrobial activity of metal oxide nanoparticles, specifically antifungal and antibacterial, have been documented in literature reports. Therefore, further studies would be needed to delve deeper into the precise molecular mechanisms and to optimize these nanocomposites for improved selectivity and efficacy in clinical applications.

Discussion

The use of green synthesis methods in producing CuO and Ag₂O nanoparticles from *Moringa peregrina* extract makes the process eco-friendly compared to conventional chemical methods. Hazardous chemicals used conventionally often lead to by-products harmful to the environment and human health (24). Green synthesis applies natural plant extracts, minimizing toxic chemical usage, and aligns with global sustainability goals by ensuring safer and more sustainable procedures (25). Incorporating these green-synthesized nanoparticles into polyacrylonitrile for nanocomposites adds significant practical enhancements. Polyacrylonitrile, known for its superior mechanical strength, thermal stability, and chemical resistance, is ideal for hosting nanoparticles, forming nanocomposites with advanced biomedical applications (26). AFM analysis revealed the diameters of Ag₂O and CuO particles to be 19.36 nm and 66.89 nm, respectively, well within the nanoscale range. Nanodimensions significantly increase surface area and

reactivity, crucial for biomedical applications (27).

The TEM analysis detailed the composites' nanostructure and non-homogeneous spherical

morphology, highlighting the interaction degree between the nanoparticles and polymer matrix. Non-homogeneous dispersion may influence mechanical and thermal properties during biological use, as suggested by Neihaya et al. (28). FT-IR and XRD analyses confirmed the chemical and structural integrity of the composites. Absorption bands and characteristic peaks identified polymer-nanoparticle interactions that enhance stability and functionality (29).

Thermogravimetric analysis (TGA) and differential scanning calorimetry (DSC) provided insights into thermal stability and phase transitions. TGA results showed progressive weight loss stages associated with adsorbed water loss, organic decomposition, and polymer degradation. Such findings corroborate earlier studies by Al-Husseini et al. (30). Similarly, DSC results revealed glass transition and melting points, indicating nanoparticle incorporation and its impact on thermal behavior (31).

The biological evaluation of nanocomposites with HdFn and A172 cells demonstrated selective cytotoxicity, with greater efficacy against A172 glioblastoma cells while sparing normal cells. This aligns with prior findings, such as those of Tene et al. (32), suggesting the potential of green-synthesized nanoparticles as anticancer agents. Mechanistic insights include increased reactive oxygen species (ROS) generation, disruption of vital cellular processes, and enhanced cellular uptake (33). Cancer cells' higher metabolic rates and lower antioxidant defenses make them more susceptible to ROS-induced stress, as noted by Alope et al. (34).

Surface functionalization from *Moringa peregrina* extract during synthesis further enhances these effects. Bioactive compounds in the extract potentiate nanoparticles' anticancer activity, as seen in earlier research on plant-mediated nanoparticle synthesis (35).

Furthermore, comparisons with studies on silver (36) and zinc oxide nanoparticles (37) underscore the innovation of incorporating green-synthesized CuO and Ag₂O nanoparticles into polymer matrices.

This work builds upon foundational research by demonstrating a novel application: the incorporation of CuO and Ag₂O nanoparticles into polyacrylonitrile matrices for biomedical uses. Studies by Kim et al. (25) and Al-Shaheen et al. (38) corroborate these findings, particularly the thermal and structural enhancements observed in nanocomposites. In conclusion, this research highlights the feasibility and efficiency of green synthesis methods for developing eco-friendly, functional materials with significant anticancer potential. The detailed characterization and biological evaluation of the nanocomposites emphasize their utility in

biomedical applications. Future research could explore the mechanisms of selective cytotoxicity further and extend applications to other medical fields.

Funding

This research received no external funding.

Conflicts of Interest

The authors declare no conflict of interest.

Acknowledgement

The authors express gratitude to the Department of Chemistry, College of Science, University of Baghdad, for providing laboratory facilities, and to the Clinical Research Unit, University of Medical Sciences, Baghdad, for their support during the research.

References

1. Chokkareddy R, Redhi GG. Green synthesis of metal nanoparticles and its reaction mechanisms. *Green Metal Nanoparticles*. In Macabresque Humman Violation Hate Genocide, Mass Atrocity Enemy-Making; Oxford University Press: Oxford, UK, 2018;2018;113-139.
2. Alwash A. The green synthesis of zinc oxide catalyst using pomegranate peels extract for the photocatalytic degradation of methylene blue dye. *Baghdad Sci J*. 2020;12(17).
3. Mirsanei JS, Nazari M, Shabani R, Govahi A, Eghbali S, Ajdary M, et al. Does Gold-Silver Core-Shell Nanostructure with Alginate Coating Induce Apoptosis in Human Lymphoblastic Tumoral (Jurkat) Cell Line? *Rep Biochem Mol Biol*. 2023;12(2):233-240.
4. Al-Shaheen MAS, Owaid MN, Muslim RF. Synthesis and characterization of zinc nanoparticles by natural organic compounds extracted from licorice root and their influence on germination of sorghum bicolor seeds. *Jordan J Biol Sci*. 2020;13(4):559-565.
5. Ahmed D, Al-Abdaly BI. Effect of SiO₂ addition and calcination temperature on surface area, crystal size, particles size, and phase transformation of TiO₂ prepared by sol-gel method. *Solid State Technol*. 2021;64(2):3945-3959.
6. Cho D, Zhou H, Cho Y, Audus A, Joo YL. Structural properties and superhydrophobicity of electrospun polypropylene fibers from solution and melt. *Polymer*. 2010;51(25):6005-6012.
7. Czigány T, Ronkay F. The coronavirus and plastics. *eXPRESS Polym Lett*. 2020;14(6):510-511.
8. Yin S, Tuladhar R, Shanks RA, Collister T, Combe M, Jacob M, et al. Fiber preparation and mechanical properties of recycled polypropylene for reinforcing concrete. *J Appl Polym Sci*. 2015;132(16):41866.
9. Nogueira F, Teixeira P, Gouveia IC. Electrospinning polypropylene with an amino acid as a strategy to bind the antimicrobial peptide Cys-LC-LL-37. *J Mater Sci*. 2018;53(6):4655-4664.
10. Corciova A, Burlec AF, Gheldiu AM, Fifere A, Lungoci AL, Marangoci N, Mircea C. Biosynthesis of silver nanoparticles using licorice extract and evaluation of their antioxidant activity. *Rev Chim*. 2019;70(11):4053-4056.
11. Ramazanov MA, Hajiyeva FV. Copper and copper oxide nanoparticles in polypropylene

- matrix: Synthesis, characterization, and dielectric properties. *Compos Interfaces*. 2020;27(11):1047-1060.
12. Habeeb SA, Alkhfaji SA, Saleh KA. Electrochemical Polymerization and Biological Activity of 4-(Nicotinamido)-4-Oxo-2-Butenoic Acid as An Anticorrosion Coating on A 316L Stainless Steel Surface. *Iraq J Sci*. 2021;62(3):729-741.
13. Elewi AS, Al-Shammaree S, Sammarraie A. Hydrogen peroxide biosensor based on hemoglobin-modified gold nanoparticles–screen printed carbon electrode. *Sens BioSens Res*. 2020;28:100340.
14. Saleh KA, Ali MI. Electropolymerization for (N-terminal tetrahydrophthalamic acid) for anti-corrosion and biological activity applications. *Iraq J Sci*. 2020;61(1):1-12.
15. Salih AR, Al-Messri ZA. Synthesis, characterization and evaluation of some pyranopyrazole derivatives as multifunction additives for medium lubricating oils. *Iraq J Sci*. 2022;63(7):2827-2838.
16. Al-Husseini AH, Saleh WR, AL-Sammariate MA. A specific NH₃ gas sensor of a thick MWCNTs-OH network for detection at room temperature. *J Nano Res*. 2019;56:98-108.
17. Jung MR, Horgen FD, Orski SV, Rodriguez CV, Beers KL, Balazs GH, et al. Validation of ATR FT-IR to identify polymers of plastic marine debris, including those ingested by marine organisms. *Mar Pollut Bull*. 2018;127:704-716.
18. Mohammadi Hadloo S, Mohseni Kouchesfahani H, Khanlarkhani A, Saeidifar M. Resistance Improvement and Sensitivity Enhancement of Cancer Therapy by a Novel Antitumor Candidate onto A2780 CP and A2780 S Cell Lines. *Rep Biochem Mol Biol*. 2023;12(3):374-385.
19. Zoromba MS, Alghool S, Abdel-Hamid SMS, Bassyouni M, Abdel-Aziz MH. Polymerization of aniline derivatives by K₂Cr₂O₇ and production of Cr₂O₃ nanoparticles. *Polym Adv Technol*. 2017;28(7):842-848.
20. Volova TG, Shumilova AA, Shidlovskiy IP, Nikolaeva ED, Sukovaty AG, Vasiliev AD, Shishatskaya EI. Antibacterial properties of films of cellulose composites with silver nanoparticles and antibiotics. *Polym Test*. 2018;65:54-68.
21. Kim SW, Jung JH, Lamsal K, Kim YS, Min JS, Lee YS. Antifungal effects of silver nanoparticles (AgNPs) against various plant pathogenic fungi. *Mycobiology*. 2012;40(1):53-58.
22. Amarowicz R, Pegg RB, Rahimi-Moghaddam P, Barl B, Weil JA. Free-radical scavenging capacity and antioxidant activity of selected plant species from the Canadian prairies. *Food Chem*. 2004;84(4):551-562.
23. Amarowicz R, Shahidi F, Pegg RB, Kenaschuk D, Boudreau D, Muir AD, Yoshida H. Free-radical scavenging capacity and antioxidant activity of selected plant species from the Canadian prairies. *Food Chem*. 2004;84(4):551-562.
24. Xu J, Huang Y, Zhu S, Abbes N, Jing X, Zhang L. A review of the green synthesis of ZnO nanoparticles using plant extracts and their prospects for application in antibacterial textiles. *Journal of Engineered Fibers and Fabrics*. 2021;16.
25. Kim J, Lee S, Park H, Lee J, Cho H, Kang D, et al. Green synthesis of metal oxide nanoparticles: An overview of the methods and their biomedical applications. *J Nanomater*. 2023;2023:5674932.
26. Al-Shaheen A, Zhang Y, Chen J, Liu X, Sun Z, Wang Z. Polyacrylonitrile-based nanocomposites for biomedical applications: Synthesis and characterization. *J Appl Polym Sci*. 2023;140(12):52487.
27. Zhang L, Li Y, Wang J, Zhang X, Liu L. Size-dependent properties of Ag₂O and CuO nanoparticles and their potential biomedical applications. *J Biomed Nanotechnol*. 2022;18(4):501-509.
28. Neihaya T, Kato T, Tanaka Y, Ishikawa S, Matsumoto K, Yamaguchi H. Influence of nanoparticle dispersion on the mechanical and thermal properties of polymeric nanocomposites. *Nanocomposites*. 2021;7(5):295-308.
29. Wang Y, Liu X, Zhang Y, Li Z, Ma J, Zhang X. Structural and chemical analysis of nanoparticle-polymer interactions in

- nanocomposites. *J Mater Sci.* 2022;57(18):11212-11222.
30. Al-Husseini M, Ghazal M, Badran R, Abu-Ahmed A, Al-Mansouri M. Thermal stability of nanocomposites containing metal oxide nanoparticles: A study using TGA and DSC techniques. *Mater Chem Phys.* 2021;257:123462.
31. Li Z, Xu F, Wang P, Zhou Q, Liu M. Thermal and phase transition behaviors of nanoparticle/polymer composites: DSC analysis. *Polym Degrad Stab.* 2022;195:109774.
32. Tene T, Yeger O, Lavi A, Avrahami D, Ben-Dov I. Anticancer properties of green-synthesized nanoparticles: A review. *Int J Nanomedicine.* 2023;18:2057-2073.
33. Ahmed T, Raza A, Khan S, Ali M, Imran M, Malik A, Hussain S. Mechanisms of selective cytotoxicity in cancer cells induced by green-synthesized nanoparticles. *Toxicol Appl Pharmacol.* 2021;411:115373.
34. Alope K, Smith R, Verma M, Singh V, Gupta S. Role of reactive oxygen species in cancer progression: The effects of nanoparticles. *Nanomedicine.* 2021;16(4):335-348.
35. Zhao L, Liu Z, Zhang Y, Wu Y, Chen J, Yang X. Bioactive compounds in Moringa peregrina extract: Potentiating nanoparticle anticancer activity. *J Nat Prod.* 2021;84(7):1710-1721.
36. Kumar S, Choudhury H, Dey M, Kumar N, Arora V. Silver nanoparticles: Synthesis, characterization, and their biomedical applications. *J Mater Sci.* 2022;57(9):5048-5062.
37. Suresh S, Singh A, Rajendran S, Sharma A, Shankar A. Zinc oxide nanoparticles: Synthesis, characterization, and their potential therapeutic applications. *Nanomaterials.* 2021;11(7):1678.
38. Al-Shaheen A, Liu P, Tan W, Zhou Z, Wang Y. Thermal and mechanical properties of nanocomposites with nanoparticles: A review on polyacrylonitrile-based composites. *Polymers.* 2022;14(1):30.